/

Paper No. 255. (quote when citing this article)
Eleventh World Conference on Earthquake Engineering
ISBN: 0 08 042822 3

SEISMIC MITIGATION OF OFFSHORE PLATFORM WITH HDR ISOLATORS

H. H. LEE
Department of Marine Environment, National Sun Yat-sen University,
Kaohsiung 800, Taiwan

ABSTRACT

The research described in this paper involves a method to mitigate the vibration of an offshore platform system in the marine environment when subjected to strong ground motions. A typical offshore platform system dynamically enhanced by the HDR devices, which was simulated by an appropriate analytical model, was analyzed and the vibration mitigation effect was evaluated. The HDR devices applied here were tested and verified that they have high energy absorption capacity. In the analysis, the applied wave forces are based on the Morrison equation for small body and the computation method is based on Newmark method for nonlinear system. Results of the vibration responses for the system with HDR devices are presented and compared to the responses of platform in the traditional design when subjected to the ground motion simulating to a typical earthquake. It was observed that the effect of the vibration mitigation and the dynamic performance of the offshore platform system could be effectively improved when the HDR devices were appropriately designed and applied.

KEYWORDS

Offshore structure, dynamic analysis, HDR isolator, seismic mitigation.

INTRODUCTION

When structures are subjected to dynamic loadings tremendous amounts of energy are input into the structural system usually. In order to mitigate the vibration and then avoid serious damage, a number of isolating systems have been developed and incorporated in the structural system. One of them is the lead-rubber bearing, a device combined with lead and layered rubbers and steel shims first developed in New Zealand in the late 1970s. Since then extensive testing has been carried out for the mechanical properties of the lead-rubber bearings (Robinson and Tucker 1981; Built 1982; Tyler and Robinson 1984). Studies for the structures with lead-rubber bearings were also performed and reduction in the system displacement was generally obtained (Lee and Medland 1978a, 1978b; Kelly and Hodder 1982). A similar seismic isolator with high-damping rubber (HDR) was developed and tested (Iemura *et al.* 1991; Tanzo *et al.* 1992). This HDR device is much thinner compared to the traditional designed isolators and the results from pseudo-dynamic testing showed that HDR isolators worked effectively for the bridge system.

As we know, typical environmental loadings exerted on the offshore structures such as the overwater wind, surface waves, strong currents and strong ground motions during severe earthquakes, usually cause significant vibrations. Severe deflections and deformations occur subsequently and then result in structural damage. Template structure is a common type of infra-structure being widely used for the offshore platform system. Therefore, in this study, a typical template structure was redesigned with HDR devices and analyzed correspondingly when subjected to a step loading and the strong ground motions. The purposes of this study are to develop an appropriate method for the application of the HDR isolators to the offshore platform systems and further to find the seismic mitigation effect by using the developed material model and the application of the particular isolator element in the nonlinear analysis.

FINITE ELEMENT FORMULATION OF THE HDR ISOLATORS

In order to adequately predict the behavior of a structural material subjected to dynamic loading, an analytical model must be capable of representing the typical material characteristics and adequately describing the dynamic behavior. A hysteretic model based on the Viscoplastic mechanical model and modified with the restoring force model (Wen, 1976; Baber and Wen, 1981), capable of accounting for the degradation of stiffness and strength and the strain hardening effect, representing a relationship between the first time derivative of the stress $d\tau/dt$ and the strain rate $\dot{\gamma}$, is presented as

$$\frac{d\tau}{dt} = \rho_k G_0 \left[\dot{\gamma} + \rho_p(\mathcal{X} - \mathcal{Y})|\dot{\gamma}| - (\rho_{s1}|\dot{\gamma}|\mathcal{Y}^n + \rho_{s2}\dot{\gamma}|\mathcal{Y}|^n)/\rho_f\right], \qquad n = 1, 3, 5, \ldots \tag{1}$$

where G_0 is the original shear modulus of the nonlinear system, and $\mathcal{X}$ and $\mathcal{Y}$ are the dimensionless strain and stress proportional to the yielding strain and stress respectively. $\rho_\bullet$'s are parameters to account for the nonlinear hysteretic characteristics. In terms of the dissipated energy, $\Xi = \int^t \tau d\gamma$, the parameters accounting for the degradation of the stiffness, strength and the nonlinearity of the loops such as ρ_k, ρ_f, ρ_p and ρ_{s1} are given as

$$\rho_\bullet = \alpha_\bullet + \beta_\bullet \exp(-\Delta_\bullet \Xi) \tag{2}$$

while

$$\rho_{s2} = -(1 - \rho_{s1}) \tag{3}$$

where $\alpha_\bullet$'s and $\beta_\bullet$'s are parameters corresponding to the orginal and the ultimate value for the data related, and $\Delta_\bullet$'s are parameters corresping to the rate of the variation of the nonlinear hysteretic characteristics. These parameters are determined from the experimental testing results and a list for the parameters corresponding the HDR isolators under study was shown in Table 1.

Parameters	α	β	Δ
ρ_k	0.50	0.50	0.01
ρ_p	0.20	-0.10	0.01
ρ_{s1}	2/3	1/3	0.01

Table 1

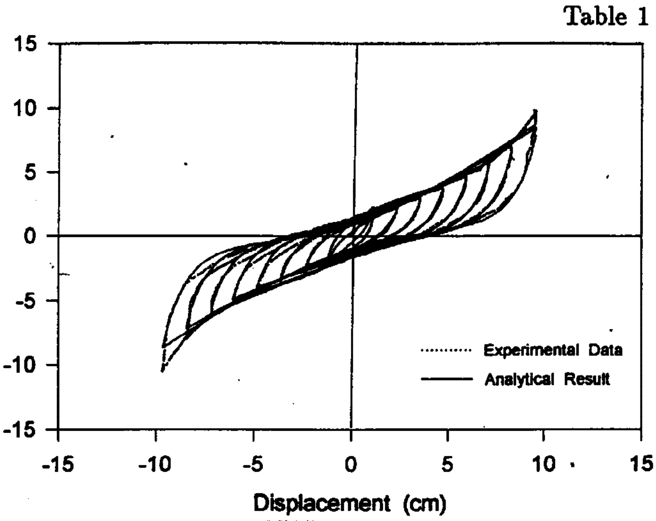

Fig.1 Comparison of the hysteretic loop between analytical and experimental results

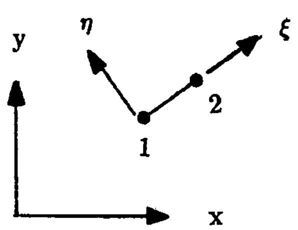

Fig.2 Two-Node HDR isolator elements

A comparison between the experimental data (according to Tanzo *et al.* 1992) and the analytical results were shown in Fig.1, where very good agreements were obtained.

Now with the analytical material model ready a 2-D finite element formulation for the HDR isolators was derived here. Since the HDR isolators are working mostly in a shear motion, the element derived here is similar to a joint element. Shown in Fig.2 are the global coordinate system x and y, and local coordinate system ξ and η. The global displacements at nodal points 1 and 2 are $\mathbf{D_1(t)}$ and $\mathbf{D_2(t)}$, respectively:

$$\mathbf{D_1(t)} = \begin{pmatrix} a_1(t) \\ a_2(t) \\ a_3(t) \end{pmatrix} \tag{4}$$

and

$$\mathbf{D_2(t)} = \begin{pmatrix} a_4(t) \\ a_5(t) \\ a_6(t) \end{pmatrix} \tag{5}$$

where $a_1(t)$ and $a_2(t)$ are global displacements at nodal point 1 in x- and y-directions respectively; $a_4(t)$ and $a_5(t)$ are those at nodal point 2 while $a_3(t)$ and $a_6(t)$ are the rotation at nodal point 1 and nodal point 2 respectively. As shown in Fig.2 the displacements in the transverse direction of the local coordinate system, η_1 and η_2, are

$$\eta_1\mathbf{(t)} = \mathbf{TD_1(t)} \tag{6}$$

and

$$\eta_2\mathbf{(t)} = \mathbf{TD_2(t)} \tag{7}$$

where $\mathbf{T}$ is a transformation matrix related to local and global coordinate systems.

The relative displacement between node 1 and 2 in the tranverse direction of the local coordinate system is defined as

$$\Delta\eta\mathbf{(t)} = \eta_2\mathbf{(t)} - \eta_1\mathbf{(t)} = \mathbf{TD_2(t)} - \mathbf{TD_1(t)} \tag{8}$$

or in the matrix form:

$$\Delta\eta\mathbf{(t)} = \mathbf{BX(t)} \tag{9}$$

where

$$\mathbf{B} = [-\mathbf{T}\ \mathbf{T}] \tag{10}$$

and

$$\mathbf{X(t)} = \begin{pmatrix} \mathbf{D_1(t)} \\ \mathbf{D_2(t)} \end{pmatrix} = \begin{pmatrix} a_1(t) \\ a_2(t) \\ a_3(t) \\ a_4(t) \\ a_5(t) \\ a_6(t) \end{pmatrix} \tag{11}$$

The engineering shear strain of the isolator considered here is given as

$$\gamma\mathbf{(t)} = \frac{\Delta\eta\mathbf{(t)}}{\mathbf{h}} \tag{12}$$

where h is the thickness of the HDR isolator. Using the virtual work principle, the equilibrium resisting force, $\mathbf{F(t)}$ resulted from the HDR isolator is given by

$$\mathbf{F(t)} = \mathbf{B^T}\tau(t)\mathbf{A_s} \tag{13}$$

where $\mathbf{A_s}$ is the shear area of the HDR isolators and shear stress τ is obtained by solving equation (1).

STRUCTURAL SYSTEM IN THE MARINE ENVIRONMENT

The dynamic equation of motion for the engineering structural member with mass $\mathbf{M}$, structural damping $\mathbf{C}$, and stiffness $\mathbf{K}$, subjected to the wave forces propagated in the normal direction η of the structural member as shown in Fig.2, can be written as

$$\mathbf{M}(\ddot{\mathbf{X}}(\mathbf{t})+\ddot{\mathbf{X}}_{\mathbf{g}}(\mathbf{t}))+\mathbf{C}\dot{\mathbf{X}}(\mathbf{t})+\mathbf{K}\mathbf{X}(\mathbf{t})=\mathbf{P}(\mathbf{t}) \tag{14}$$

where $\ddot{\mathbf{X}}(\mathbf{t})$, $\dot{\mathbf{X}}(\mathbf{t})$ and $\mathbf{X}(\mathbf{t})$ are the acceleration, velocity and displacement relative to the ground motion respectively and $\ddot{\mathbf{X}}_{\mathbf{g}}(\mathbf{t})$ is the ground acceleration. Taking into account of the relative motion between the structures and fluids, the wave forces exerted on the body, $\mathbf{P}(\mathbf{t})$ (Newman 1977, Isaacson 1979) are

$$\mathbf{P}(\mathbf{t})=\rho C_m V^e\dot{\mathbf{U}}_{\mathbf{n}}(\mathbf{t})-\rho C_a V^e(\ddot{\mathbf{X}}_{\mathbf{n}}(\mathbf{t})+\ddot{\mathbf{X}}_{\mathbf{gn}}(\mathbf{t}))+\frac{1}{2}\rho C_d A^e|\mathbf{U}_{\mathbf{n}}(\mathbf{t})-\dot{\mathbf{X}}_{\mathbf{n}}(\mathbf{t})|(\mathbf{U}_{\mathbf{n}}(\mathbf{t})-\dot{\mathbf{X}}_{\mathbf{n}}(\mathbf{t})), \tag{15}$$

where $C_a=C_m-1$, and $\mathbf{U}_{\mathbf{n}}(\mathbf{t})$ and $\dot{\mathbf{U}}_{\mathbf{n}}(\mathbf{t})$ are the velocity and acceleration of the fluid normal to the structural member resulted from the horizontal and vertical motion of the fluid, respectively. $\ddot{\mathbf{X}}_{\mathbf{n}}(\mathbf{t})$ and $\dot{\mathbf{X}}_{\mathbf{n}}(\mathbf{t})$ are the acceleration and the velocity of the structural member relative to the ground in the normal direction η, and $\ddot{\mathbf{X}}_{\mathbf{gn}}(\mathbf{t})$ is the ground acceleration in the normal direction η. C_m and C_d are coefficients corresponding to inertia and drag effect respectively. V^e and A^e are the displaced volume and the projected front area of the structural member, respectively. The last term in the equation representing the drag force due to the relative velocity of fluid is nonlinear. The nonlinearity of the drag term is retained through the use of the approximate relation derived by Penzien and Tseng(1978),

$$|\mathbf{U}_{\mathbf{n}}(\mathbf{t})-\dot{\mathbf{X}}_{\mathbf{n}}(\mathbf{t})|(\mathbf{U}_{\mathbf{n}}(\mathbf{t})-\dot{\mathbf{X}}_{\mathbf{n}}(\mathbf{t}))=|\mathbf{U}_{\mathbf{n}}|\mathbf{U}_{\mathbf{n}}(\mathbf{t})-2<|\mathbf{U}_{\mathbf{n}}|>\dot{\mathbf{X}}_{\mathbf{n}}(\mathbf{t}), \tag{16}$$

where $<|\mathbf{U}_{\mathbf{n}}|>=\hat{\mathbf{U}}_{\mathbf{n}}$ represents the time average of $|\mathbf{U}_{\mathbf{n}}|$. Through the substitution of Equation (16), Equation (15) then becomes

$$\mathbf{P}(\mathbf{t})=\rho C_m V^e\dot{\mathbf{U}}_{\mathbf{n}}(\mathbf{t})-\rho C_a V^e(\ddot{\mathbf{X}}_{\mathbf{n}}(\mathbf{t})+\ddot{\mathbf{X}}_{\mathbf{gn}}(\mathbf{t}))+\frac{1}{2}\rho C_d A^e\left(|\mathbf{U}_{\mathbf{n}}|\mathbf{U}_{\mathbf{n}}(\mathbf{t})-2\hat{\mathbf{U}}_{\mathbf{n}}\dot{\mathbf{X}}_{\mathbf{n}}(\mathbf{t})\right), \tag{17}$$

Now the normal motion for both structural displacements and fluids at the nodes of the structural member can be transformed into the global system, respectively, as

$$\mathbf{X}_{\mathbf{n}}(\mathbf{t})=\mathbf{B}_1\mathbf{X}(\mathbf{t}) \tag{18}$$

and

$$\mathbf{U}_{\mathbf{n}}(\mathbf{t})=\mathbf{B}_1\mathbf{U}(\mathbf{t}) \tag{19}$$

After the substitution of Equations (17), (18) and (19), Equation (14) takes the form as

$$\tilde{\mathbf{M}}^{\mathbf{e}}\ddot{\mathbf{X}}(\mathbf{t})+\tilde{\mathbf{C}}^{\mathbf{e}}\dot{\mathbf{X}}(\mathbf{t})+\mathbf{K}^{\mathbf{e}}\mathbf{X}(\mathbf{t})=\tilde{\mathbf{C}}^{\mathbf{e}}_{\mathbf{m}}\dot{\mathbf{U}}(\mathbf{t})+\tilde{\mathbf{C}}^{\mathbf{e}}_{\mathbf{d}}\mathbf{U}(\mathbf{t})-\tilde{\mathbf{M}}^{\mathbf{e}}\ddot{\mathbf{X}}_{\mathbf{g}}(\mathbf{t}) \tag{20}$$

where

$$\tilde{\mathbf{M}}^{\mathbf{e}}=\mathbf{M}+\rho C_a V^e\mathbf{B}_1; \tag{21}$$

$$\tilde{\mathbf{C}}^{\mathbf{e}}=\mathbf{C}+\rho C_d A^e\hat{\mathbf{U}}_{\mathbf{n}}\mathbf{B}_1; \tag{22}$$

$$\tilde{\mathbf{C}}^{\mathbf{e}}_{\mathbf{m}}=\rho C_m V^e\mathbf{B}_1; \tag{23}$$

$$\tilde{\mathbf{C}}^{\mathbf{e}}_{\mathbf{d}}=\frac{1}{2}\rho C_d A^e|\mathbf{U}_{\mathbf{n}}|\mathbf{B}_1 \tag{24}$$

Now if the HDR devices are applied, a nonlinear force induced by the HDR isolators might be added to the structural system, and after the combination of equations for each element to the whole system the equations of motion take a form as

$$\tilde{\mathbf{M}}\ddot{\mathbf{X}}(t) + \tilde{\mathbf{C}}\dot{\mathbf{X}}(t) + \tilde{\mathbf{K}}\dot{\mathbf{X}}(t) + \mathbf{F}(t) = \tilde{\mathbf{P}}(t). \quad (25)$$

where $\tilde{\mathbf{M}}$ and $\tilde{\mathbf{C}}$ are global mass and damping matrix respectively As a customary application due to the uncertainty of the system damping, the damping matrix of the system may be simplified as

$$\tilde{\mathbf{C}} = 2\zeta\omega_n\tilde{\mathbf{M}}; \quad (26)$$

Now having the equations of motion and the forces exerted on the structural system ready, the analysis can be carried out by using the step-by-step integration schemes for the nonlinear structural system such as Newmark-β method (Newmark 1962), Wilson's method (Bathe and Wilson 1976) and etc.. In this study the Newmark method using average acceleration operator was adopted due to its stability advantage.

NUMERICAL RESULTS AND DISCUSSION

In the numerical analysis, a typical template platform of 5-story and 2-bay was designed and shown in Fig.3. The outer diameter and the thickness of the vertical pile is 4 *ft.* and 1.5 *in.* respectively, and 2*ft.* and 0.5 *in.* for the other structural members. The platform was assumed clamped on the sea floor and the density of the structural material and water were 15.2 $slugs/ft^3$ and 1.99 $slugs/ft^3$ respectively. The mass was uniformly distributed on the deck and assumed to be 58,680 *slugs*.

The HDR isolator applied in this study is adopted from Tanzo's study in which the isolator is 25x25 cm^2 in plan and 4.8 cm high and the axial bearing pressure is 64 kg/cm^2 with 200% maximum strain allowed. The isolators were installed between the top deck of the platform and the infra-structures as shown in Fig.3. In order to have an axial bearing pressure compatible to the experimental results, the total shear area was 4x4 ft^2 for each set of isolators while the thickness remained unchanged. The analysis was focused on the displacement induced by the input loading and the effect of displacement reduction when the HDR isolators were applied. The results were obtained by carrying out the calculation for the coupled MDOF nonlinear system, and then plotted and represented in figures.

In the first analysis a step ground motion of 0.1 g was input while the wave force and system damping were ignored, and the maximum strain of the isolator was confined to 100%. The response of the middle isolator was shown in Fig.4 and comparison for the top deck displacment was shown in Fig.5 when the platform system subjected to step loading. In the second analysis the maximum strain of the isolator was confined to 200% and a ground motion as shown in Fig.6 similar to 1940 El Centro earthquake was input. Fig.7 showed the response of the isolator and Fig.8 respresented the comparison for the displacement response of the top deck. A stress-strain curve respresented the HDR isolator mechanic behavior during the earthquakes was shown in Fig.9 and Fig.10 for the first and second 10 seconds respectively.

CONCLUSIONS

As was shown in the analysis, it is realized that with appropriate application of the HDR isolator the offshore structure might have better dynamic performance. When subjected to step loadings the top deck shifts to one side but its vibration amplitude is reduced. When subjected to a loading similar to the earthquakes the reduction of the displacement response is more significant. From the hysterstic loops of the HDR isolator it showed that the isolator worked effectively in dissipating the input energy.

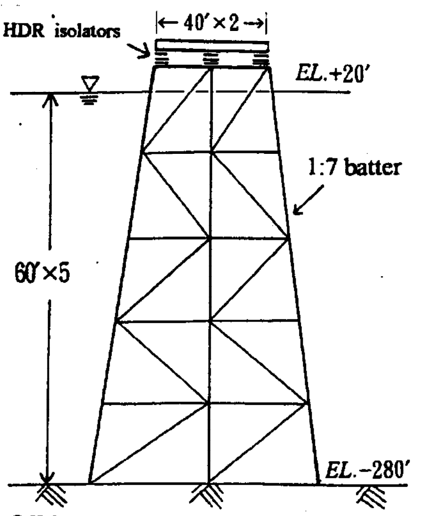

Fig.3 Offshore platform incorporated with HDR

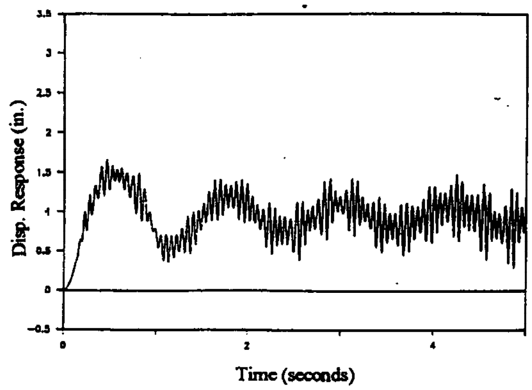

Fig.4 Response of HDR isolators for step-loading

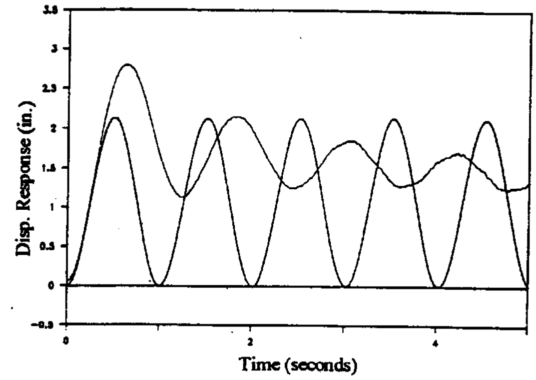

Fig.5 Response comparison of top deck for step-loading

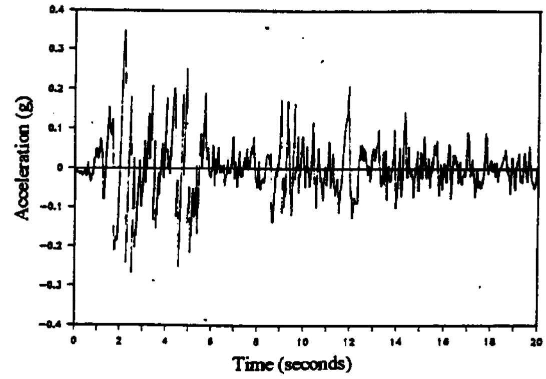

Fig.6 N-S component of ground motion, El- Centro (1940)

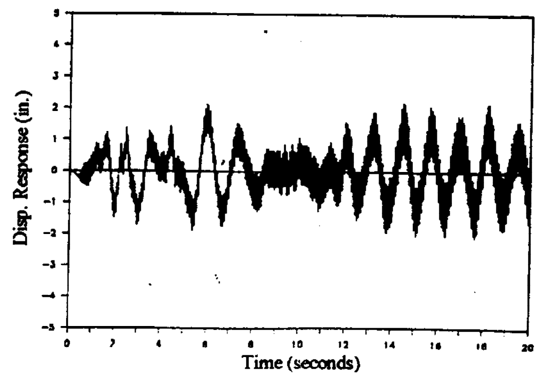

Fig.7 Response of HDR isolators for El-Centro Earthquake

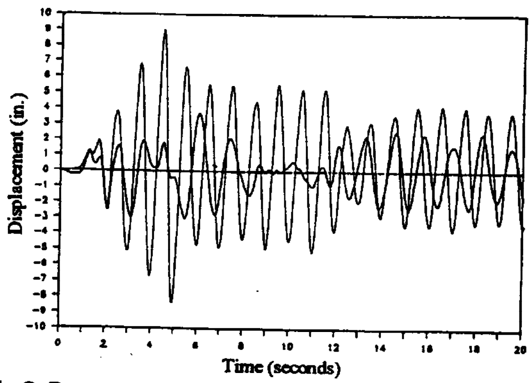

Fig.8 Response comparision of top deck for Earthquake

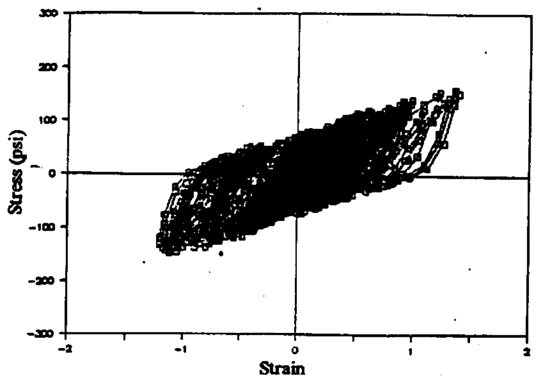

Fig.9 Stress-strain curve of HDR isolators (0~10 secs.)

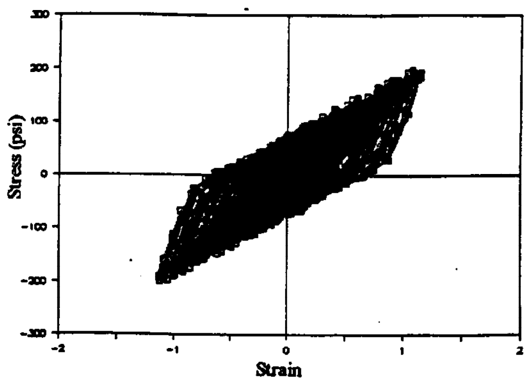

Fig.10 Stress-strain curve of HDR isolators (10~20 secs.)

REFERENCES

Baber, T.T. and Wen, Y.K.(1981). Random vibration of hysteretic, degrading system. *J. Engrg. Mechanics Div.* ASCE, Vol. 107, No. EM6, pp 1069-1087.

Built, S.M. (1982). Lead rubber dissipators for the base isolation of bridge structures, *School of Engrg. Rept.*. No.28, Dept. Civil Engrg., Univ. Auckland.

Bathe, K.J. and Wilson, E.L.(1976).*Numerical methods in finite element analysis.* Prentice-Hall, Englewood Cliffs, NJ

Iemura, H., Yamada Y., Tanzo, W., Uno, Y. and Nakamura, S. (1991). On-line earthquake response tests of high-damping rubber bearings for seismic isolation, Us-Japan Seminar on Earthquake Protective Systems, Buffalo N.Y.

Isaacson, M. (1979). Nonlinear inertia forces on bodies. *J. Waterways etc.* Div. ASCE, No.WW3,pp.213-227.

Kelly, J.M. and Hodder, S.B.(1982). Experimental study of lead and elastomeric dampers for base isolation systems in laminated neoprene bearings,*Bull. New Zealand Natl. Soc. Earthquake Engrg.*, No.15 (2), pp 53-67.

Lee, D.M. and Medland, L.C.(1978a). Base isolation- An historical development, and the influence of higher mode responses,*New Zealand Natl. Soc. Earthquake Engrg.*, No.11 (4), pp 219-233.

Lee, D.M. and Medland, L.C.(1978b). Estimation of base isolated structure responses, *New Zealand Natl. Soc. Earthquake Engrg.*, No.11 (4), pp 234-244.

Newmark, N.M. (1962). A method of computation for structural dynamics. *Trans.* ASCE, Vol.127,pt.1, pp.1406-1435.

Penzien, J. and Tseng, S. (1978). Three-Dimensional Dynamic Analysis of Fixed Offshore Platforms. In *Numerical Methods in Offshore Engineering*, John Wiley and Sons, New York, pp.221-243.

Robinson, W.H. and Tucker, A.G. (1981). Test results for lead-rubber bearings for Wm. Clayton Building, Toe Toe Bridge, and Waiotukupuna Bridge, *Bull. New Zealand Natl. Soc. Earthquake Engrg.*, No.14 (1), pp 21-33.

Tanzo, W., Yamada, Y., Uno, Y. and Nakamura, S.(1992) *Proceedings* 10th World Conference on Earthquake Engineering, 19-24 July/Madrid, Spain pp 2233-2236

Tyler, R.G. and Robinson, W.H. (1984). High strength tests on lead rubber bearings for earthquake loadings, *Bull. New Zealand Natl. Soc. Earthquake Engrg.*, No.17 (2), pp 90-105.

Wen, Y.K.(1976). Method for random vibration of hysteretic systems, *J. Engrg. Mechanics Div.* ASCE, Vol.102, No.EM2, pp 249-263.